Molecular Biology of the Cell
Vol. 21, 334–344, January 15, 2010

Basic Fibroblast Growth Factor Elicits Formation of Interstitial Axonal Branches via Enhanced Severing of Microtubules

Liang Qiang, Wenqian Yu, Mei Liu, Joanna M. Solowska, and Peter W. Baas

Department of Neurobiology and Anatomy, Drexel University College of Medicine, Philadelphia, PA 19129

Submitted September 30, 2009; Revised November 6, 2009; Accepted November 12, 2009
Monitoring Editor: Paul Forscher

The formation of interstitial axonal branches involves the severing of microtubules at sites where new branches form. Here we wished to ascertain whether basic fibroblast growth factor (bFGF) enhances axonal branching through alterations in proteins involved in the severing of microtubules. We found that treatment of cultured hippocampal neurons with bFGF heightens expression of both katanin and spastin, which are proteins that sever microtubules in the axon. In addition, treatment with bFGF enhances phosphorylation of tau at sites expected to cause it to dissociate from microtubules. This is important because tau regulates the access of katanin to the microtubule. In live-cell imaging experiments, axons of neurons treated with bFGF displayed greater numbers of dynamic free ends of microtubules, as well as greater numbers of short mobile microtubules. Entirely similar enhancement of axonal branching, short microtubule transport, and frequency of microtubule ends was observed when spastin was overexpressed in the neurons. Depletion of either katanin or spastin with siRNA diminished but did not eliminate the enhancement in branching elicited by bFGF. Collectively, these results indicate that bFGF enhances axonal branch formation by augmenting the severing of microtubules through both a spastin-based mode and a katanin-based mode.

INTRODUCTION

A typical vertebrate neuron extends a single axon that branches extensively in order to innervate multiple targets. This can occur either via bifurcation of the growth cone at the tip of the parent axon, or via the formation of interstitial (also called "collateral") branches along the length of the parent axon. Although the former predominates in cultures of PNS neurons, interstitial branching appears to be the primary mode by which axons arborize during development and in cultures of CNS neurons. The formation of an interstitial branch involves dynamic interplay between the microtubules in the parent axon and the cortical actin cytoskeleton (Dent and Kalil, 2001). The most dramatic cytoskeletal event that occurs during branch formation appears to be the focal severing of the long microtubules that dominate the axonal shaft into a concentration of numerous very short microtubules that are able to transit into the newly forming branch (Yu *et al.*, 1994; Dent *et al.*, 1999). This is critical because the newly forming branch needs a robust supply of incoming microtubules (Yu *et al.*, 1994), because only very short microtubules in the axon are mobile (Wang and Brown, 2002) and because an enrichment of plus ends of microtubules is important for interacting with a variety of proteins and cortical structures relevant to axonal branching (Kornack and Giger, 2005).

There are two microtubule-severing enzymes that have been studied extensively in neurons, namely katanin and spastin (Yu *et al.*, 2007; Falnikar and Baas, 2009). Recently, we and others documented that overexpression of spastin in cultured rat hippocampal neurons markedly enhances the formation of axonal branches, whereas depletion of spastin markedly diminishes branch frequency (Yu *et al.*, 2008; Riano *et al.*, 2009). The story with katanin was not as simple, as overexpression of katanin did not enhance branch formation (Yu *et al.*, 2005). However, we found that katanin's access to the microtubule is regulated by tau (Qiang *et al.*, 2006) and that depletion of tau can cause enhancement of axonal branching through a katanin-based mechanism (Yu *et al.*, 2008). Therefore we proposed that axons can branch through either a katanin-based mode involving tau or a spastin-based mode that appears to be independent of tau. The existence of both modes provides redundancy but also may provide different levels of control, in response to growth factors that regulate axonal branching at different developmental stages or under different circumstances.

Basic fibroblast growth factor (bFGF) is one of the most potent inducers of axonal branch formation (Szebenyi *et al.*, 2001; Aletsee *et al.*, 2003; Klimaschewski *et al.*, 2004). When applied to neuronal cultures, bFGF causes a marked increase in branch frequency that is apparent within a day of application. Little is known, however, about the specific changes elicited by bFGF that give rise to branching. Here, we wanted to test the hypothesis that bFGF alters the levels and/or regulation of proteins relevant to the severing of microtubules. We also wanted to ascertain whether bFGF stimulates axonal branching through the katanin-based mode, the spastin-based mode, or both. Finally, we investigated whether experimental augmentation of microtubule severing produces similar effects on microtubule behaviors as treatment of the neurons with bFGF.

This article was published online ahead of print in *MBC in Press* (http://www.molbiolcell.org/cgi/doi/10.1091/mbc.E09–09–0834) on November 25, 2009.

Address correspondence to: Peter W. Baas (pbaas@drexelmed.edu).

MATERIALS AND METHODS

Cell Culture and Transfection

Cultures of rat hippocampal neurons were prepared as previously described (Qiang *et al.*, 2006; Yu *et al.*, 2008). DNA constructs were transfected into the dissociated neurons before plating, using the Amaxa Nucleofector (Amaxa Biosystems, Köln, Germany). After nucleofection, the neurons were plated onto poly-L-lysine–treated glass coverslips as previously described (Qiang *et al.*, 2006; Yu *et al.*, 2008). For some experiments, the coverslips were also coated with laminin after the polylysine treatment because this was found to promote faster and straighter growth of axons. bFGF (Promega, Madison, WI, Cat. no. 9PIG507) was applied to some of the neuronal cultures at a concentration of 20 ng/ml (Szebenyi *et al.*, 2001). DNA constructs included enhanced green fluorescent protein (EGFP)-α-tubulin (Clontech, Palo Alto, CA), EGFP-EB3 (provided by Dr. Niels Galjart, Erasmus Medical Center), and mCherry-spastin (prepared in our laboratory). For the spastin construct, we used the M85 isoform of spastin, which is the predominant isoform expressed in developing neurons (Claudiani *et al.*, 2005; Connell *et al.*, 2008; Mancuso and Rugarli, 2008; Solowska *et al.*, 2008; Yu *et al.*, 2008). For controls, we used the appropriate constructs for EGFP or/and mCherry. For studies involving siRNA, neurons were transfected with a pool of four sequences specific to rat spastin, p60-katanin, or p80-katanin (purchased as "smartpools" from Dharmacon, Boulder, CO, Accession numbers: XM-343018, L-080249-01, and M-092761-00, respectively) or with a nonspecific control sequence (Dharmacon, Cat. no. D-001206-03-20). Transfections with the siRNA smartpools were performed using the Nucleofector as previously described (Yu *et al.*, 2005, 2008; Qiang *et al.*, 2006). After 2 d in culture to permit protein depletion, the neurons treated with siRNA were replated so that neurites could grow anew in the near absence of the relevant protein targeted by the siRNA.

Microtubule Transport Assay

To image the transport of microtubules in axons, the neurons were transfected with EGFP-α-tubulin. In some experiments, control neurons (not treated with bFGF) were compared with neurons treated with bFGF. In other cases, control neurons (expressing mCherry) were compared with neurons expressing mCherry-spastin. The latter was to ascertain any potential changes elicited by spastin overexpression. In other experiments, neurons were transfected with control or spastin siRNA and then transfected with the EGFP-α-tubulin construct 2 d later and then replated. To assist in monitoring transport of microtubules over relatively long and straight trajectories, the neurons were plated onto poly-L-lysine with laminin (see above). Imaging was conducted 24–48 h after plating or replating. Individual unfasciculated axons with clearly identifiable directionality of growth from the cell body were chosen for analysis so that anterograde and retrograde movements could be identified with certainty. We used the Zeiss inverted Observer Z1 microscope (Carl Zeiss, Jena, Germany), with a Zeiss incubation chamber, interfaced with the MicroPoint Mosaic Digital Diaphragm system from Photonics Instruments (St. Charles, IL), coupled to an argon ion laser. The Zeiss incubation chamber provides optimal culture conditions of 37°C and 5% CO_2. The photonic laser Mosaic system was used to photobleach regions of the axons in similar manner to our earlier studies on microtubule transport (Hasaka *et al.*, 2004; He *et al.*, 2005; Ahmad *et al.*, 2006; Myers and Baas, 2007). Only one photobleached region was made on each axon analyzed. This region was always 40–50 μm in length and always was located roughly equidistant from the cell body and the tip of the axon. A 100× 1.3 NA Plan Apo oil immersion objective and a GFP filter set (Chroma Technology, Brattleboro, VT) were used for acquiring fluorescence images. The CCD camera and most aspects of the microscope were controlled by Axiovision 4.1 software (Zeiss) running on an Intel Xeon processor-based computer (Fujitsu Siemens, Berlin, Germany) with the Windows XP Professional operating system (Microsoft, Seattle, WA). The intensity of epifluorescence illumination was attenuated to 30% to reduce photobleaching and photodamage during acquisition; 2 × 2 binning was applied to increase signal intensity. Images were acquired at 1.8-s intervals, with ~280–320-ms exposure time. Time-lapse images were saved as "zvi" files and analyzed using Axiovision 4.1 software. Motion analysis was performed only on axons that displayed at least one microtubule that was visible without digital processing. Additional analysis was conducted using digital contrast adjustments within the "Image Properties" application of Axiovision 4.1. Statistics were performed using the Student's *t* test.

EB3 Live-Cell Imaging

To image the assembly of microtubules from their plus ends, we expressed fluorescently tagged EB3, which is a microtubule "end binding protein" that tracks with the plus ends of microtubules during bouts of rapid assembly (Stepanova *et al.*, 2003). We have used this approach in a number of our studies on microtubule behaviors in cultured neurons (Hasaka *et al.*, 2004; Ahmad *et al.*, 2006; Myers *et al.*, 2006; Nadar *et al.*, 2008). To visualize EB3 comets within the axon of the cultured neurons in the experiments involving bFGF, we transfected neurons with EGFP-EB3 and cultured in medium containing bFGF. To image EGFP-EB3 within the axons of spastin-overexpressing neurons, we cotransfected neurons with both EGFP-EB3 and mCherry-spastin. Images were acquired at a rate of 1 per second excluding camera exposure times to time-lapse movies. Depending on the fluorescence intensity of EB3, exposure time ranged from 250 to 350 ms so that the real-time imaging of individual axons ranged from 2 to 4 min. As with the microtubule transport assay described above, we used the Zeiss inverted Observer Z1 microscope with the Zeiss incubation chamber, and we analyzed only one region per axon that always located roughly equidistant from the cell body and the tip of the axon. The region we analyzed was always 50–70 μm in length, a bit longer than the length analyzed in the microtubule transport studies. Details on the objective, camera, software, illumination, and binning were also the same as described above for the microtubule transport studies. EB3 quantification was performed using Axiovision "measure" module. Numbers of EB3 comets, average speeds of the comets and longevities of the comets were analyzed in details. Frames extracted for still images were exported from Axiovision as TIFF files and processed in Photoshop 7 (Adobe Photosystems, San Jose, CA). Statistics were performed using the Student's *t* test.

Primary Antibodies Used for Western Blotting and Immunofluorescence Analyses

Primary antibodies included the following: monoclonal: tau1 (anti-dephosphorylated tau, obtained from Dr. Lester Binder of Northwest University; Binder *et al.*, 1985), tau5 (anti-total tau, also obtained from Binder; Papasozomenos and Binder, 1987), anti-β tubulin directly conjugated with Cy3 (Sigma, St. Louis, MO, Cat. no. C4585), anti-GAPDH (Ambion, Austin, TX, Cat. no. AM4300); Polyclonal: anti-spastin (AAA spastin antibody; Solowska *et al.*, 2008), tauR1 (anti-total tau, obtained from Binder; Berry *et al.*, 2004), anti-P60-katanin (Yu *et al.*, 2005), anti-P80-katanin (Yu *et al.*, 2005), and anti-GFP (Abcam, Cambridge, MA, Cat. no. ab6556).

Western Blotting

Western blotting was conducted as in our previous studies for siRNA experiments, to ensure that over 95% of the spastin protein had been depleted before the replating step (Qiang *et al.*, 2006; Yu *et al.*, 2008). Western blotting was also used for experiments aimed at ascertaining changes in the levels of various proteins during treatment of neurons with bFGF. For the latter, Western blotting was conducted on cultures that had been exposed to bFGF for 4, 24, or 72 h.

Immunofluorescence Analyses

Procedures of the immunofluorescence studies were performed as previously described (Yu *et al.*, 2005, 2008; Qiang *et al.*, 2006). For the experiments on microtubule distribution after experimental manipulations, the cultures were simultaneously fixed and extracted 24–48 h after plating. For the experiments relevant to the ratio images of tau1/tauR1, the cultures were fixed and then extracted after fixation 24–72 h after plating. Primary antibodies against proteins of interest (same as used for the Western blotting, see above; except that we used the polyclonal antibody tauR1 for staining total tau) were applied followed by appropriate secondary antibodies. Images (except those using tau1 and tauR1 antibodies) were obtained on an Axiovert 200M microscope (Carl Zeiss) equipped with a high-resolution CCD (Orca, Hamamatsu, Japan). The images were obtained using identical camera, microscope, and imaging criteria such as gain, brightness and contrast, and exposure time. In some cases, fluorescence images were subjected to the "invert" function in Adobe Photoshop (San Jose, CA) that converts blacks to whites and whites to blacks and inverts gray levels proportionally, because we found that fine details were more clearly visualized. The resulting images are referred to as "inverted images." In one set of studies, ratio images were generated of cultures double-labeled with tau1 and tauR1 antibodies using the Pascal confocal microscope. Statistics were performed using the Student's *t* test.

RESULTS

bFGF Increases the Frequency of Microtubule Transport in the Axon

The goal of the first set of experiments was to test whether the axons of neurons treated with bFGF display a greater frequency of microtubule transport. This would presumably occur if there were higher numbers of microtubules (resulting from microtubule severing) short enough to undergo transport. Live-cell imaging studies of microtubules in the axons of cultured rat sympathetic neurons (from the superior cervical ganglia of newborn rat pups) have consistently shown that only very short microtubules, roughly 7 μm or less, are mobile (Wang and Brown, 2002; Ahmad *et al.*, 2006). The present studies are the first to use the photobleach assay for microtubule transport on cultured hippocampal neurons. We have found that when using this assay on sympathetic neurons, it is highly advantageous to grow them on

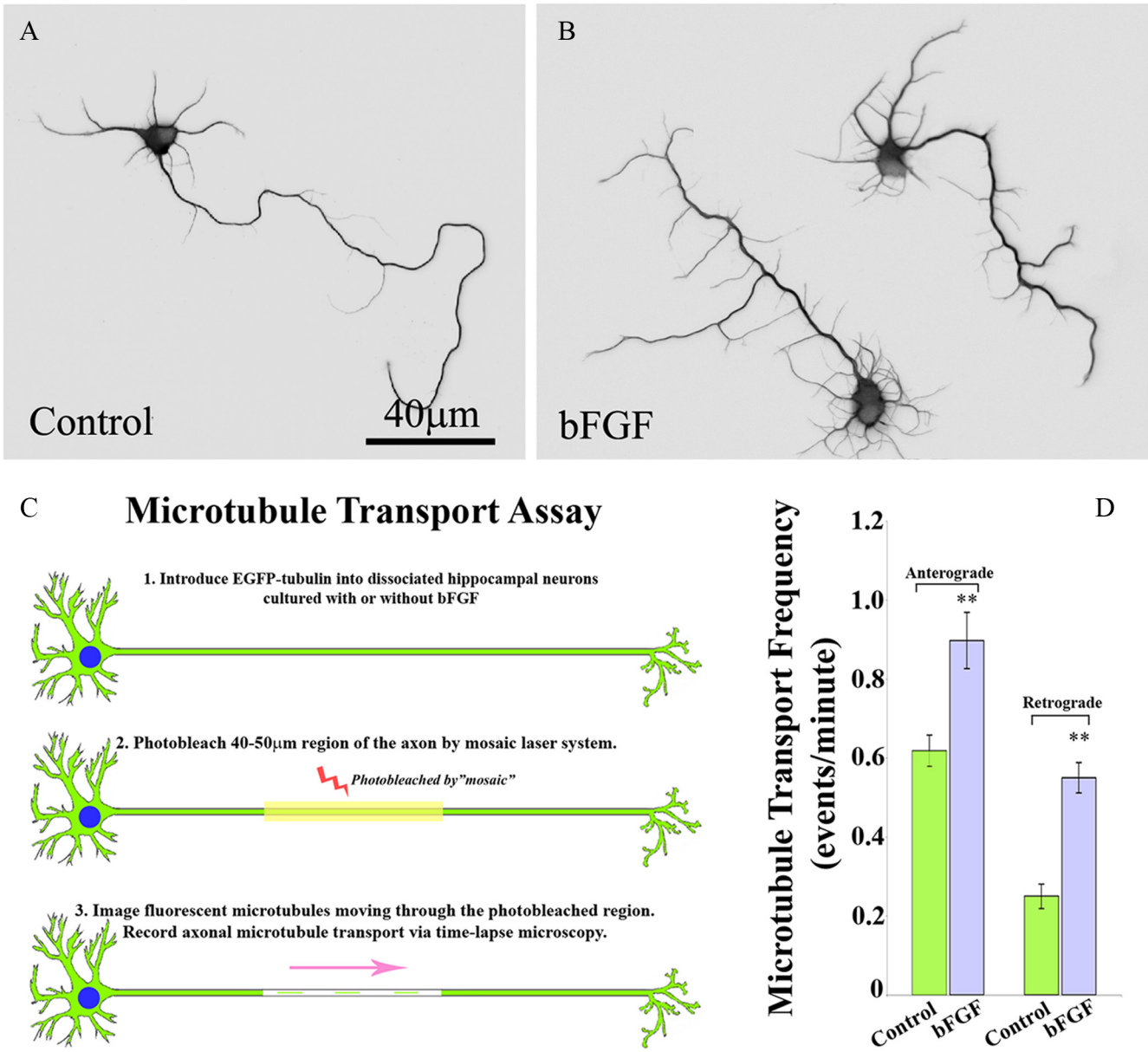

Figure 1. bFGF alters the morphology of hippocampal neurons and microtubule transport in the axon. (A and B) Immunostains of microtubules in cultured hippocampal neurons. To reveal cellular morphology in greater detail, cells are displayed as inverted images. (A) Control neuron. (B) Neurons treated with bFGF (20 ng/ml). (C) Schematic diagram of the microtubule transport assay. (D) Quantitative analyses of the frequencies of microtubule transport in both anterograde and retrograde directions. In control neurons, 71% of the microtubule transport events are in the anterograde direction. The frequencies of both anterograde and retrograde microtubule transport are significantly increased in the presence of bFGF (anterograde by 45%, $p < 0.01$; retrograde by more than 120%, $p < 0.001$). Scale bar, 40 μm.

laminin, because the axons grow faster and straighter and are generally thinner in diameter, compared with axons grown on polylysine without laminin. We found the same to be true of hippocampal neurons. Importantly, the bFGF-induced branching effect remained similar with or without laminin. Figure 1, A and B, show examples of control neurons and neurons treated with bFGF for 48 h; a marked increase in axonal branching is apparent. Figure 1C shows a schematic diagram of the procedure for assaying microtubule transport, which is essentially the same as we used previously except that we are now using the Mosaic system for performing the photobleaching (see *Materials and Methods*).

For each experimental case, we imaged 40 different axons. We focused on unbranched regions of the axon because regions giving rise to new branches would presumably show increases in microtubule severing and transport regardless of whether or not the neuron had been treated with bFGF. We previously documented that, in the axons of control sympathetic neurons, the ratio of the frequency of anterograde microtubule transport to retrograde microtubule transport is 2:1 (Hasaka *et al.*, 2004; He *et al.*, 2005). In the axons of control hippocampal neurons, there was an even greater bias in the anterograde direction, with a ratio of 2.5:1 (anterograde, 71%; retrograde, 29%). When bFGF was applied to the culture, the total number of anterograde mi-

crotubule transport events was significantly increased. In control axons there were 0.618 ± 0.039 transport events/min in the anterograde direction, whereas in bFGF-treated axons there were 0.898 ± 0.071 transport events/min in the anterograde direction. This is a 45% increase in transport events ($p < 0.01$). Retrograde transport was displayed as 0.250 ± 0.031 and 0.551 ± 0.038 transport events/min ($p < 0.01$) in control and bFGF-treated axons, respectively (120% increase, Figure 1D). Thus, the ratio of anterograde to retrograde microtubule transport dropped to ~1.6:1 in bFGF-treated hippocampal neurons.

In pursuing these experiments, we noticed that not only does bFGF elicit more axonal branches, but also it significantly enhances the number of immature neurites ("minor processes") that grow from the cell body (Figure 1, A and B). This is relevant to the issue of microtubule severing because we have documented in previous studies that manipulation of proteins relevant to microtubule severing can affect the number of immature neurites as well as the branching of the axon (Yu *et al.,* 2005, 2008). These observations may reflect a mechanistic and perhaps evolutionary link between process number and axonal branching as means for enhancing the complexity of the neuritic arbor of a developing neuron.

bFGF Increases the Number and Duration of Microtubule Plus-End Assembly Events in the Axon

We would expect the severing of microtubules not only to create more short mobile microtubules but would also to create more dynamic plus ends of microtubules within the axonal shaft. To explore the effects of bFGF on the number, distribution and dynamic behavior of microtubule plus ends in the axon, we visualized fluorescent "comets" at the plus ends of microtubules generated by expression of EGFP-EB3 in the neurons. EB3 is a member of a category of proteins called TIPs that associate with microtubule plus ends during bouts of rapid assembly (Stepanova *et al.,* 2003; Kornack and Giger, 2005; Wu *et al.,* 2006). The excursion of the EGFP-EB3 at the plus end of the microtubule appears as a moving comet because the EB3 gradually dissociates from the tubulin subunits after their addition to the plus end of the microtubule, thus producing a comet-shaped burst of fluorescence with its tail toward the minus end of the microtubule. The number of comets was quantified per 100 μm of axonal length. In control axons, the average numbers of EB3 comets were 22.37 ± 0.497 in the anterograde direction and 1.78 ± 0.129 in the retrograde direction, respectively. Both numbers were significantly augmented when bFGF was added into the culture ($p < 0.001$). The average numbers were 34.31 ± 0.938 (53.4% increase relative to control) in the anterograde direction and 6.78 ± 0.267 (281.1% increase relative to control) in the retrograde direction (Figure 2, A, D, and E, Movies 1–3). Interestingly, the greater increase in the retrograde comets was even more accentuated at sites within the parent axon that were giving rise to new branches. However, in the newly forming branches themselves, EB3 comets only moved anterogradely (Figure 2F and Movie 3).

Regarding the velocity of EB3 comets, we did not detect any significant difference between anterograde and retrograde comets in each group ($p > 0.05$, Figure 2B, Movies 1 and 2). However, we detected a slight increase in the duration of both anterograde and retrograde EB3 comets in bFGF-treated axons (10.14 ± 0.610 s, anterograde; 10.07 ± 0.485 s, retrograde; $p < 0.05$), comparing to those in controls (8.83 ± 0.361 s, anterograde; 8.77 ± 0.435 s, retrograde, Figure 2C, Movies 1 and 2). The longer durations suggest that bFGF-treatment not only generates more microtubule plus ends but it also affects the dynamic properties of the microtubules as well.

bFGF Impacts Proteins Related to Microtubule Severing

As noted earlier, application of bFGF results in higher numbers of immature processes as well as higher numbers of axonal branches (Figure 1). Given that experimental manipulation of proteins relevant to microtubule severing can have these same two effects on neurons (Yu *et al.,* 2005, 2008), this observation provides provocative initial evidence that a key effect of bFGF may be to alter the expression or activity of these proteins. To investigate this, we analyzed the effects of bFGF on spastin and P60-katanin. In addition, we included two other proteins in these analyses, namely tau and P80-katanin. Tau binds along the surface of the microtubule and suppresses the capacity of P60-katanin (and spastin, to a much lesser extent) to access the microtubule lattice (Qiang *et al.,* 2006; Yu *et al.,* 2008). P80-katanin is a protein that interacts with P60-katanin in a manner that can augment its microtubule-severing properties (McNally *et al.,* 2000). To investigate the effects of bFGF on these four proteins, cultured hippocampal neurons were allowed to grow axons for 24–48 h, after which they were rinsed three to four times with serum-free medium. After rinsing, bFGF-containing serum-free medium was added for 4, 24, and 72 h before harvesting the cultures for Western blotting. With regard to tau, we used two monoclonal different antibodies: one called tau5, which recognizes all tau, and the other called tau1, which recognizes tau only when it is dephosphorylated at certain sites that are relevant to its binding to microtubules. When tau is phosphorylated at these sites, its binding affinity to microtubules is diminished and it is no longer recognized by the tau1 antibody (Papasozomenos and Binder, 1987; Mandell and Banker, 1996).

As shown in Figure 3, the addition of bFGF causes elevations in the levels of both spastin and P60-katanin after 24 h, but does not increase the levels of P80-katanin or tau (Figure 3, A–C). However, with regard to tau, it is clear that it becomes markedly more phosphorylated as early as 4 h after addition of bFGF. Twenty-four hours later, it reaches its highest point and remains at this higher phosphorylation level even after 72 h (Figure 3, A and C). These results are consistent with a scenario whereby bFGF enhances microtubule severing first by increasing the phosphorylation of tau in a manner that causes it to dissociate from microtubules and then by increasing the levels of both P60-katanin and spastin. Expression of P80-katanin does not appear to be modified by bFGF (Figure 3, B and C).

In a recent publication, we speculated that there are two "modes" by which the neuron augments microtubule severing to elicit branch formation. We called these the katanin-mode and the spastin-mode (Yu *et al.,* 2008). The katanin-mode relies on the local dissociation of tau from microtubules at a site of impending branch formation, which enables P60-katanin to focally sever microtubules in that vicinity. The spastin-mode is not dependent on changes in tau, but rather upon the accumulation of sufficient levels of spastin protein. If correct, this would mean that any one branch could form via either one of these two modes or a combination of both. Consistent with this view, spastin was observed to accumulate at some sites of branch formation, but not all (Yu *et al.,* 2008). Here, we used immunofluorescence-based ratio imaging to analyze axons with regard to tau phosphorylation. As predicted by the existence of two different modes for branching, we observed that the ratio of tau1 to total tau (tau1/tauR1; see *Materials and Methods*) was

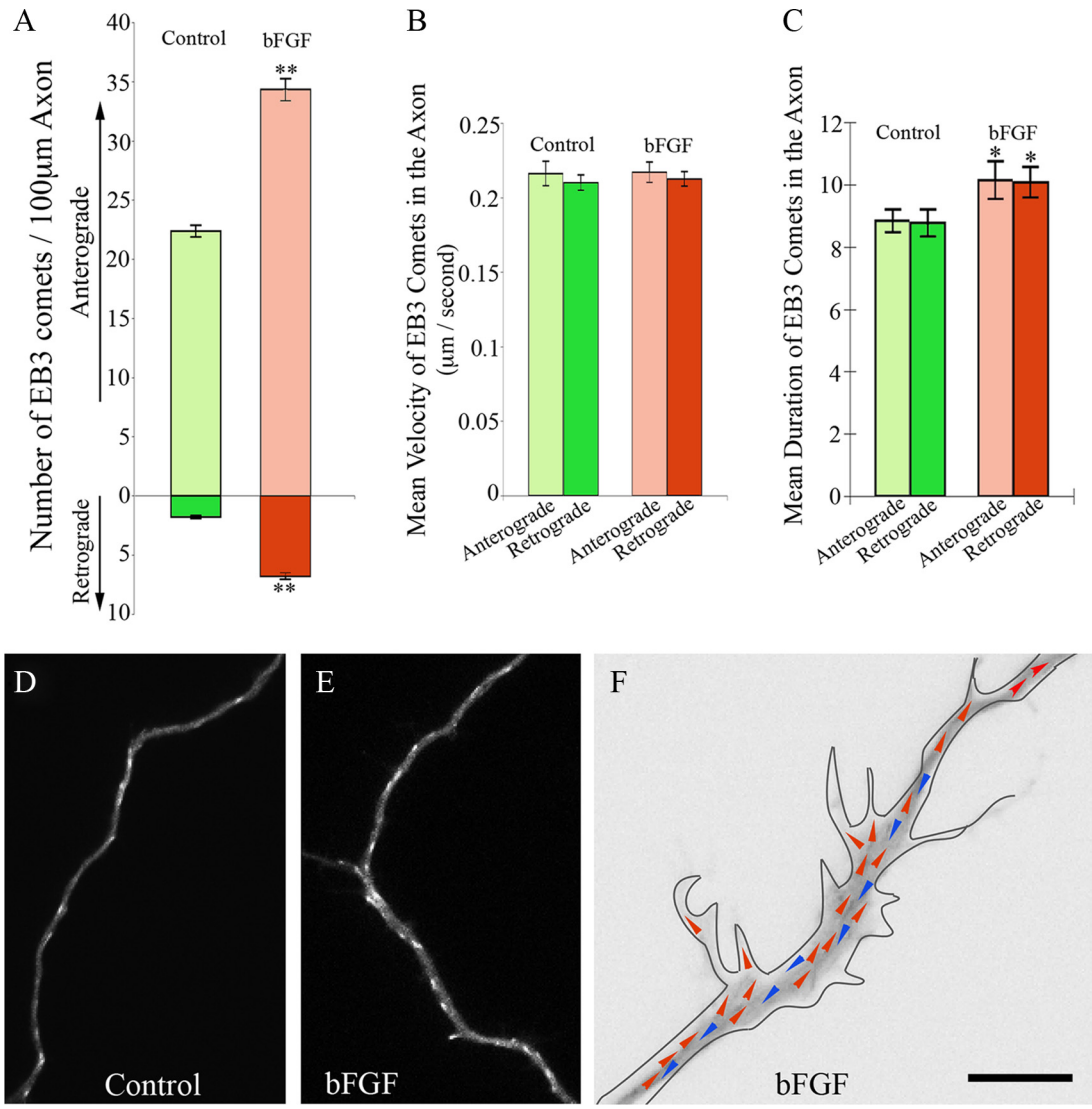

Figure 2. bFGF increases the number of EB3 comets in the axon and their average duration. (A) Quantitative analyses of the number of EB3 comets within control and bFGF-treated axons. bFGF increases the number of anterograde EB3 excursions by 53.4% ($p < 0.001$) and the number of retrograde excursions by 281.1% ($p < 0.001$). (B) Quantitative analyses of average EB3 excursion velocities within the axons of control and bFGF-treated neurons. No significant difference was detected ($p > 0.05$). (C) Quantitative analyses of average duration time of EB3 comets within control and bFGF-treated axons. There is no significant difference in duration time between the anterograde and retrograde comets in either control neurons and neurons treated with bFGF. However, bFGF enhances the duration time in both anterograde and retrograde directions by 14.8% ($p < 0.05$). (D) Still-frame image extracted from live-cell movie of a control axon expressing EGFP-EB3. (E) Still-frame image extracted from live-cell movie of an axon treated with bFGF and expressing EGFP-EB3. (F) An inverted still-frame image extracted from live-cell movies of an axon treated with bFGF and expressing EGFP-EB3. Red arrows, the anterograde EB3 excursions; blue arrows, the retrograde EB3 excursions. Scale bar, (D and E) 12 μm; (F) 5 μm. Anterograde equals upward for all (D–F).

diminished at some but not all sites of branch formation. An example is shown in Figure 4.

If the two microtubule-severing modes truly work independently of one another, we would anticipate that depleting neurons of spastin or P60-katanin via siRNA before the application of bFGF should partially but not completely eliminate the capacity of bFGF to augment axonal branching. Using our standard approach for treating neurons with siRNA (see *Materials and Methods*; Qiang *et al.*, 2006; Yu *et al.*, 2008), we determined by Western blotting that spastin, P60-katanin, and P80-katanin were depleted more than 95% by their respective siRNA smartpools (Figure 5A). When applied to control cultures, bFGF increases the number of axonal branches by almost fourfold (Figures 1, A and B, and 5F). No significant differences in neuronal morphology were detected between control neurons and neurons transfected with control siRNA. This was also true of the two groups when they were both exposed to bFGF (Figure 1, A and B, and data not shown). Therefore, neurons transfected with nonspecific siRNA were used as the control group in these experiments. When spastin was depleted from cultures not treated with bFGF, the number of axonal branches was reduced by about half. When FGF was applied to cultures depleted of spastin, the increase in axonal branches was 2.52-fold (Figure 5, Bb and F), whereas in the cultures depleted of P60-katanin, the increase was 1.70-fold (Figure 5, Cc and F). Thus, each of the two severing proteins contributes to the augmentation of axonal branching produced by bFGF.

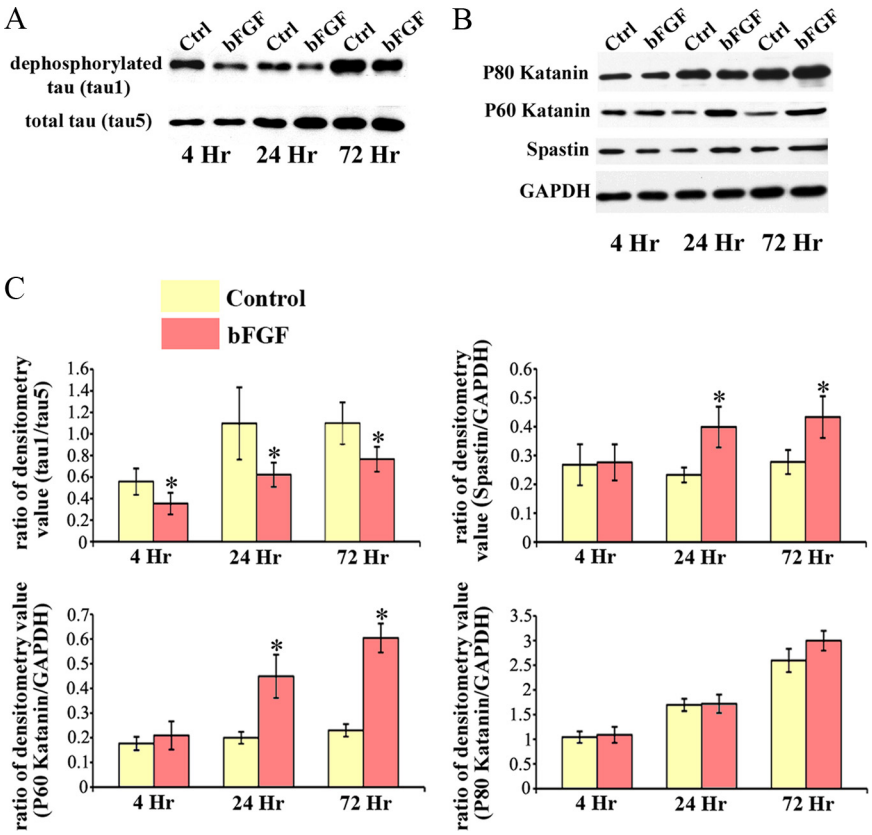

Figure 3. Profile of proteins relevant to microtubule severing is changed in the presence of bFGF. (A and B) Western blots of whole cell extracts probed with antibodies for dephosphorylated tau (tau1), total tau (tau5), P80-katanin, P60-katanin, spastin, and GAPDH. A, Tau becomes more phosphorylated with bFGF treatment (20 ng/ml), as early as 4 h. (B) Both P60-katanin and spastin are elevated after 24 h in bFGF. The levels of P80-katanin are not affected by bFGF. (C) Quantitative analysis based on the densitometry values of immunopositive bands using the Syngene imaging system. The values are expressed as arbitrary units. Final data were normalized to densitometry values of either tau5 (for studies in A) or GAPDH (for studies in B). Each bar represents the average measurements of three experiments.

The results on immature neurites were not completely the same as the results on branching. When applied to the cultures, bFGF increased the number of immature neurites by about twofold (Figures 1, A and B, and 5E). When spastin or P60-katanin was depleted from cultures not treated with bFGF the number of immature neurites remained the same (Figure 5, B, C, and E). Moreover, depletion of spastin or P60-katanin had no impact on bFGF's augmentation of neurite number (Figure 5, Bb, Cc, and E). Interestingly, depletion of P80-katanin had no apparent effect on the formation of axonal branches or immature neurites (Figure 5, Dd, E, and F). Thus, although overexpression of either spastin or

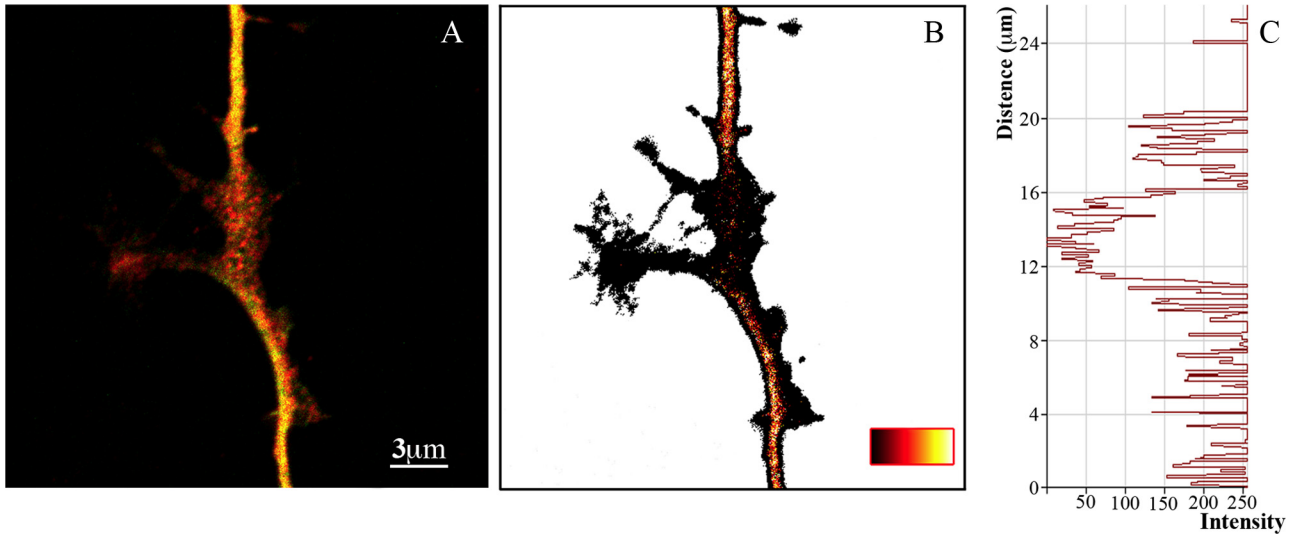

Figure 4. Tau phosphorylation is elevated in regions of impending axonal branching. (A) Overlay fluorescence images of tau1 (green) and tauR1 (red) in the axonal shaft and in a region of impending axonal branch formation. (B) Ratio image of tau1/tauR1 of panel A generated by Pascal software in pseudocolor. Low ratio is black (see bar at bottom right). (C) Quantitative intensity of a line profile through the ratio image shown in B. The site of impending branch formation displays dramatically lower ratio of tau1/tauR1 than adjacent regions of the axonal shaft. Scale bar, 4 μm.

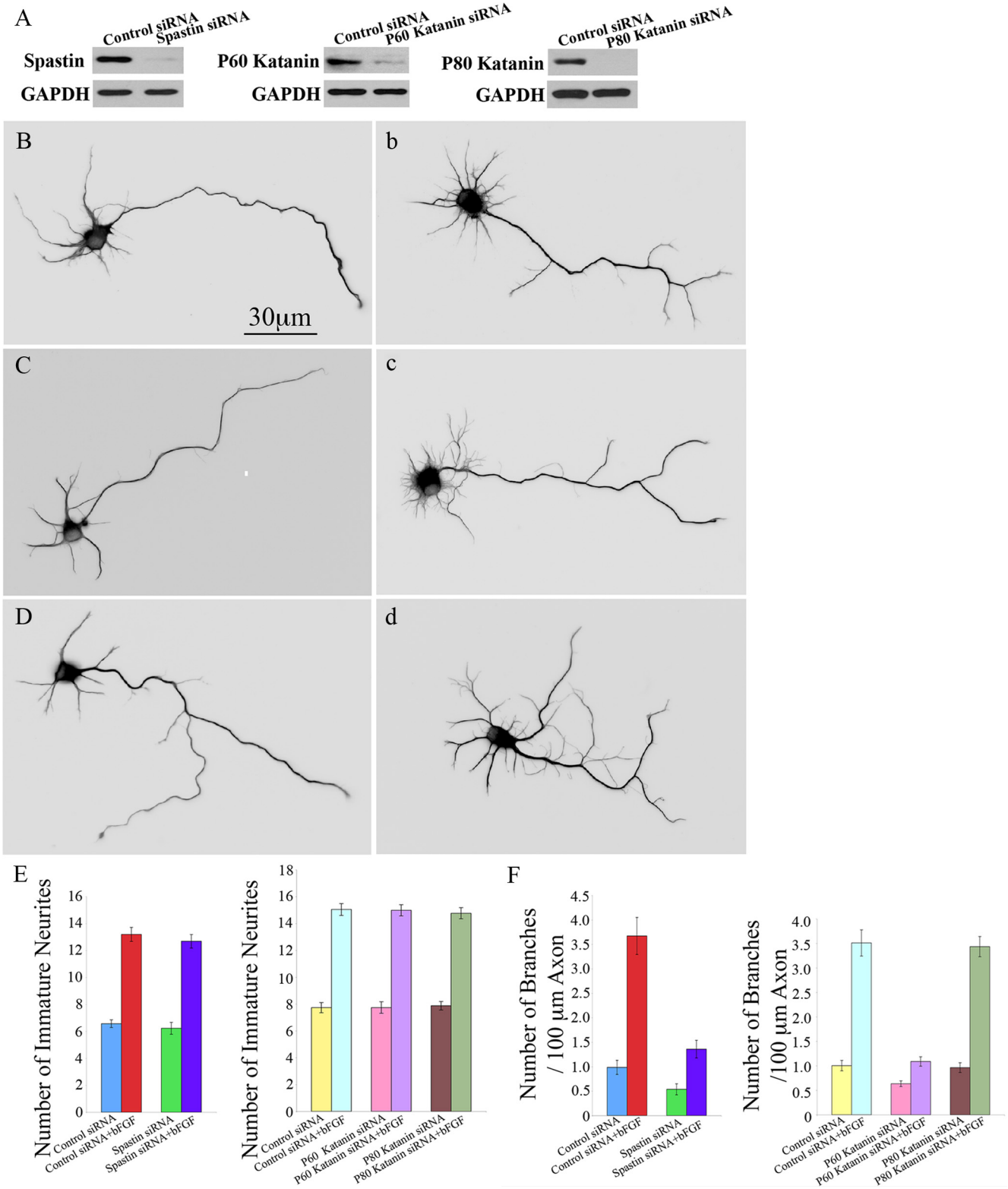

Figure 5. Morphological analyses of hippocampal neurons exposed to bFGF and depleted of spastin, P60-katanin or P80-katanin. (A) Western blots of whole cell extracts probed with antibodies for spastin, P60-katanin, and P80-katanin. Each protein was successfully knocked down in cultured of hippocampal neurons by more than 95% by the relevant siRNA smartpool. (Bb–Dd) Immunostains of microtubules in cultured hippocampal neurons. To reveal cellular morphology in greater detail, cells were displayed as inverted images. (B) Spastin-depleted neuron. (b) Spastin-depleted treated with bFGF. (C) P60-katanin–depleted neuron. (c) P60-katanin–depleted neuron treated bFGF. (D) P80-katanin–depleted neuron. (d) P80-katanin–depleted neuron treated with bFGF. (E) Quantitative analyses of the number of immature neurites of the different experimental groups. There is no significant difference between the control and the spastin-depleted group (B) ($p > 0.05$), between the control and the P60-katanin–depleted group (C) ($p > 0.05$) and between the control and the P80-katanin–depleted group

P80-katanin dramatically increases neurite number (Yu *et al.*, 2005, 2008), the presence of these proteins does not appear to be required to achieve the typical neurite number displayed either with or without bFGF.

Overexpression of Spastin Alters the Frequency of Microtubule Transport and the Behavior of EB3 Comets within the Axon

To test whether changes in microtubule transport and the behavior of EB3 comets induced by bFGF are attributed to microtubule-severing activity, we analyzed microtubule transport and the behavior of EB3 comets in axons with experimentally enhanced microtubule-severing activity. For these experiments, we overexpressed spastin rather than p60-katanin because the activity of the latter is complicated by its regulation by tau. For each experimental case, we imaged 40 different axons. When spastin was overexpressed in cultured hippocampal neurons (using mCherry wild-type spastin), the number of anterograde microtubule transport events was significantly increased compared with control axons from 0.618 ± 0.039 to 0.845 ± 0.040 events/min (37% elevation; $p < 0.001$), and the number of retrograde transport was also significantly increased from 0.250 ± 0.031–0.508 ± 0.053 events/min (103% elevation; $p < 0.001$, Figure 6). In addition, we used siRNA for spastin to evaluate whether a reduction in microtubule-severing activity would result in diminution of microtubule transport frequencies. When spastin was depleted by siRNA (which depletes over 95% of the protein, as determined by Western blotting; see Yu *et al.*, 2008 and Figure 5), the total number of anterograde microtubule transport events (0.419 ± 0.050 transport events/min, $p < 0.01$), as well as the retrograde ones (0.172 ± 0.021 transport events/min, $p < 0.01$, Figure 6), was significantly reduced by 32 and 31%, respectively.

With regard to the behavior of EB3 comets within the axon, numbers of both anterograde and retrograde comets were significantly augmented when spastin was overexpressed ($p < 0.001$). Per 100 μm of axon, there was an average of 33.73 ± 1.287 (50.8% increase) in the anterograde direction and 7.25 ± 0.395 (307.3% increase) in the retrograde direction (Figure 7, A, D, and E, and Movies 4 and 5). Similar to the bFGF-treated group, the average velocity of EB3 comets was not significantly different with the overexpression of spastin in either direction ($p > 0.05$, Figure 7B and Movies 4 and 5). However, the duration was slightly greater of both anterograde and retrograde EB3 comets in the axons overexpressing spastin (10.00 ± 0.428 s, anterograde; 10.08 ± 0.363 s, retrograde; $p < 0.05$), compared with those in controls (8.83 ± 0.361 s, anterograde; 8.77 ± 0.435 s, retrograde, Figure 7C and Movies 4 and 5).

Thus, both with regard to microtubule transport and the behavior of EB3 comets, overexpression of spastin results in changes that are remarkably similar to those observed when neurons are treated with bFGF.

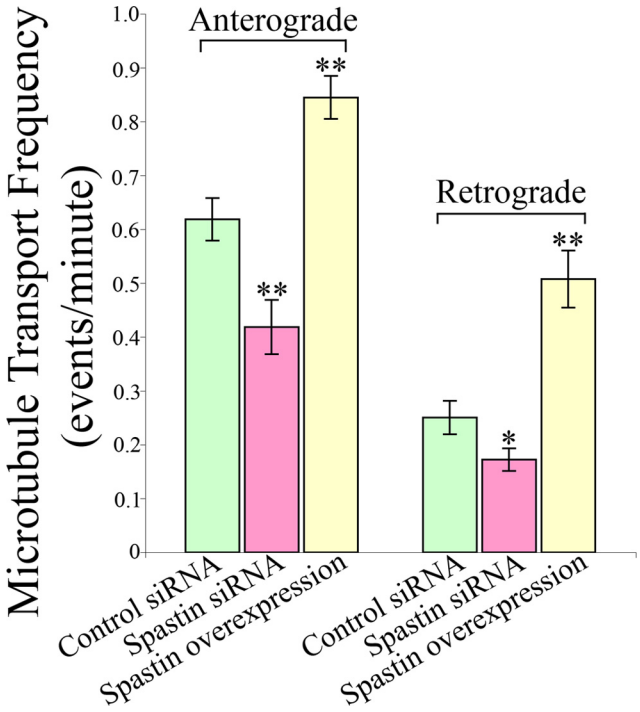

Figure 6. The frequency of microtubule transport changes when microtubule severing is experimentally enhanced or suppressed. Quantitative analyses of the frequencies of microtubule transport in both anterograde and retrograde directions. In control neurons, 71% of the microtubule transport events are in the anterograde direction. The frequencies of both anterograde and retrograde microtubule transport are significantly increased (anterograde by 37%; retrograde by over 103%; $p < 0.001$) as a result of spastin overexpression. When spastin is depleted, the frequency of anterograde microtubule transport is reduced by 32% ($p < 0.01$), as well as that of the retrograde transport by 31% ($p < 0.05$). The ratios of anterograde to retrograde transport are altered accordingly (see *Results*).

Figure 5 (cont). (D) ($p > 0.05$). Although bFGF significantly increased the number of immature neurites in the control siRNA ($p < 0.01$), spastin-depleted ($p < 0.01$), P60-katanin–depleted ($p < 0.01$) and P80-katanin–depleted groups ($p < 0.01$), no significant difference was detected between control neurons treated with bFGF and spastin-depleted neurons treated with bFGF (b) ($p > 0.05$), between control neurons treated with bFGF and P60-katanin–depleted neurons treated with bFGF (c) ($p > 0.05$) and between control neurons treated with bFGF and P80-katanin–depleted neurons treated with bFGF (d) ($p > 0.05$). (F) Quantitative analyses of the number of primary branches per 100 μm of axon of different groups under the conditions described in B, b, C, c, D, and d compared with the control. bFGF significantly increased the number of axonal branches in the control siRNA neurons ($p < 0.001$), spastin-depleted neurons (between B and b; $p < 0.01$), P60-katanin–depleted neurons (between C and c; $p < 0.01$), and P80-katanin–depleted neurons (between D and d; $p < 0.001$). There is a significant decrease of axonal branches after the depletion of spastin (B) or P60-katanin (C) in hippocampal neurons compare to control ($p < 0.01$). After being treated with bFGF, the number of axonal branches is also significantly decreased in spastin siRNA neurons compared with control (b, $p < 0.001$), as is the case with P60-katanin–depleted neurons compared with control (c, $p < 0.001$). No significant difference was detected between control and P80-katanin–depleted neurons (D, $p > 0.05$) or between control neurons treated with bFGF and P80-katanin–depleted neurons treated with FGF (d, $p > 0.05$). Scale bar, 30 μm.

DISCUSSION

In order for an interstitial branch to form, there must be a local concentration of microtubule free ends as well as an abundance of short microtubules that are able to transit into the new branch (Joshi and Baas, 1993). It is now well established that such effects are produced by microtubule severing (Dent *et al.*, 1999; Yu *et al.*, 2005, 2008; Riano *et al.*, 2009) and that P60-katanin and spastin have somewhat different severing properties (Yu *et al.*, 2008). P60-katanin chops microtubules rather unevenly, resulting in a mixture of long and short polymers, whereas spastin produces a more even

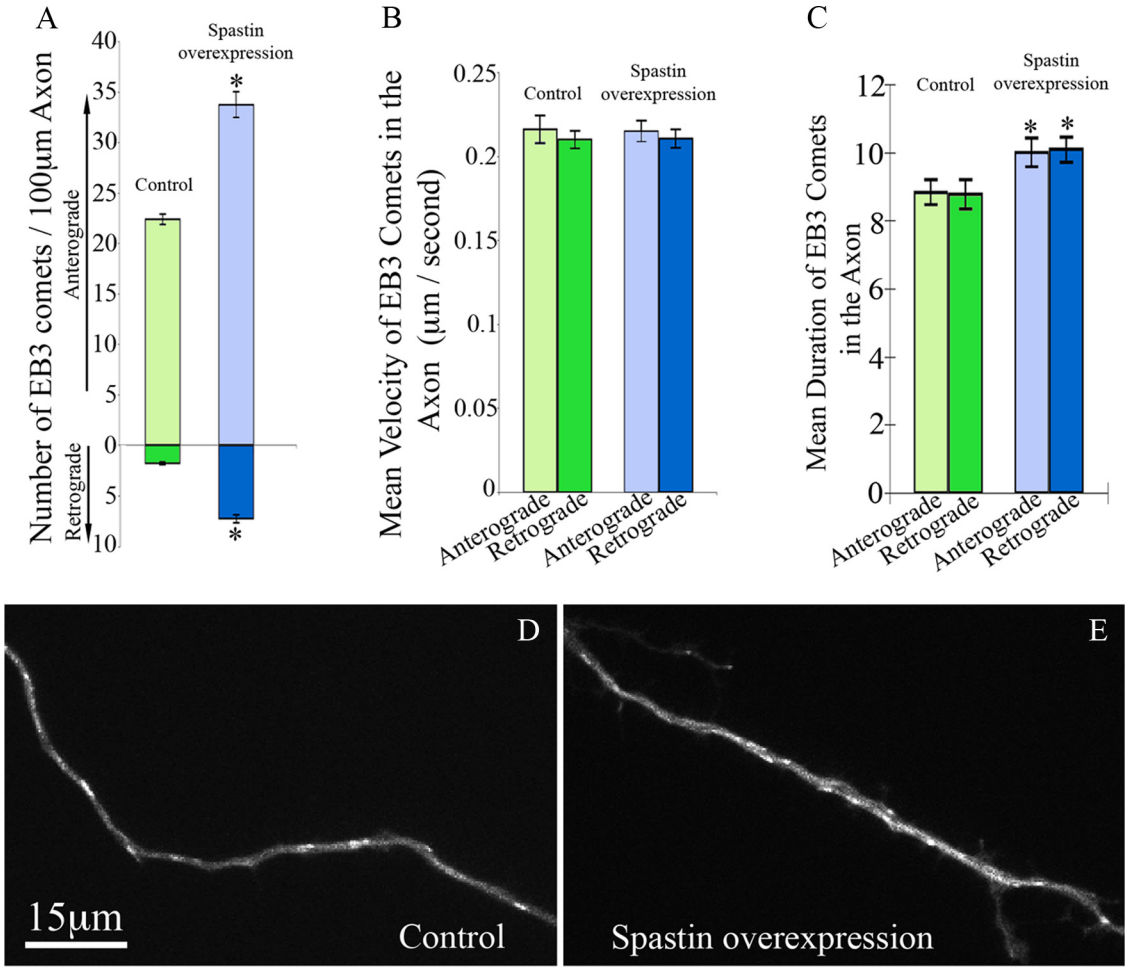

Figure 7. Overexpression of spastin alters the behavior of EB3 comets in a manner similar to bFGF. (A) Quantitative analyses of the number of EB3 comets within the axons of control neurons and neurons overexpressing spastin. Overexpression of spastin increases the number of anterograde EB3 excursion by 50.8% ($p < 0.001$), and that of retrograde by 307.3% ($p < 0.001$) relative to the control. (B) Quantitative analyses of average EB3 excursion velocities within the axons of control neurons and neurons overexpressing spastin. No significant difference was detected between each group ($p > 0.05$). (C) Quantitative analysis of average duration time of EB3 comets in the axons of control and spastin-overexpressing neurons. There is no significant difference in duration time between the anterograde and retrograde comets in either control neurons or neurons overexpressing spastin. However, overexpression of spastin enhances the duration time in the anterograde direction (by 13.3%, $p < 0.05$) and the retrograde direction (by 13.6%, $p < 0.05$). (D) Still-frame image extracted from a live-cell movie of a control axon expressing EGFP-EB3. (E) Still-frame image extracted from a live-cell movie of an axon expressing EGFP-EB3 and mCherry-spastin. Scale bar, 15 μm. The anterograde direction is toward the right for D and E.

chopping, resulting in a concentration of short microtubules. Severing of microtubules by P60-katanin is attenuated by the binding of tau to the microtubule lattice (Qiang *et al.*, 2006), but spastin is less affected by tau microtubules (Yu *et al.*, 2008). On this basis, we have proposed that there is a katanin-mode and a spastin-mode by which axons can sever microtubules to give rise to a branch. The former is dependent on tau, whereas the latter is not. There may be other modes as well, based on other severing proteins (Zhang *et al.*, 2007; Lee *et al.*, 2009).

It makes sense that neurons would have more than one option for severing microtubules. One advantage is redundancy. It is known, for example, that animals lacking spastin or tau do not display major flaws in axonal branching (Dawson *et al.*, 2001; Tarrade *et al.*, 2006). Another advantage is that each option could be utilized differently during development; for example, various growth factors relevant to axonal branching (such as slit proteins, SDF-1, or netrin-1; Wang *et al.*, 1999; Dent *et al.*, 2004; Pujol *et al.*, 2005) could elicit their effects specifically through one option or another. Here we sought to determine if altering in microtubule severing is a primary means by which bFGF elicits its effects on axonal branching, and if so, whether bFGF does so by impacting the spastin-mode, the katanin-mode, or both.

Our biochemical analyses indicate that treatment of neurons with bFGF results in a notable increase in the levels of both spastin and P60-katanin. There is no detectable increase in P80-katanin, which suggests that the activity of P60-katanin is not augmented by changes in the levels of this cofactor. However, there is a notable increase in the phosphorylation of tau at sites on the molecule that cause it to dissociate from the microtubule. Less tau bound to the microtubules would make them more sensitive to severing by P60-katanin. The conclusion that bFGF augments both modes is supported by observations that bFGF is still able to enhance branching when either spastin or katanin was depleted from the neurons.

It should be noted that, although not eliminated entirely, branching was diminished when either spastin or P60-katanin was depleted, indicating a role for each of the two proteins in regulating branching. It is curious that the depletion of P60-katanin resulted in a relatively mild phenotype compared with previous studies in which axonal formation was severely compromised by injection of a function-blocking antibody to P60-katanin (Ahmad *et al.*, 1999) or by expression of a p60-katanin dominant/negative construct (Karabay *et al.*, 2004; Yu *et al.*, 2005). One possibility is that these other experimental tools may affect other severing proteins as well as P60-katanin. For example, in order to function, P60-katanin must form a hexamer (Hartman and Vale, 1999). If other microtubule-severing proteins cohexamerize with P60-katanin, the dominant-negative approach or the function-blocking antibody would be expected to inhibit other severing proteins as well as P60-katanin. Alternatively, the milder phenotype observed with the siRNA-based depletion may be due to upregulation of other severing proteins during the gradual depletion of P60-katanin.

The live-cell imaging studies of microtubule behaviors were undertaken in light of what we call the "cut and run" model for microtubules (Baas *et al.*, 2005, 2006). The premise of this model is that molecular motor proteins are constantly tugging on microtubules of all lengths, but only transport microtubules that are sufficiently short. If this is correct, the determinative step in microtubule mobility is the severing of long microtubules into pieces short enough to be transported. This model predicts that more microtubule severing in the axon should lead to more frequent microtubule transport events, whereas less severing should lead to less frequent microtubule transport events. This prediction was born out in our observations on neurons in which spastin was either depleted or overexpressed. In the former case microtubule transport was less frequent, whereas in the latter case it was more frequent. We also observed more frequent assembly excursions with the EB3 imaging as a result of spastin overexpression, which is consistent with the expectation that enhanced severing would create more assembly-active plus ends of microtubules. Particularly interesting was the fact that treatment of neurons with bFGF caused qualitatively similar changes in microtubule behaviors as observed with spastin overexpression. Specifically, bFGF treatment enhanced the frequency of microtubule transport as well as the numbers of EB3 comets. Thus, although bFGF undoubtedly affects a variety of proteins that we have not studied here, it is notable that the phenotype produced by bFGF treatment can be closely matched by overexpression of just one protein.

The EB3 (or in some studies, EB1 has been used) approach for visualizing microtubule behaviors in the axon also reveals information on the polarity orientation of the microtubules. Anterogradely-moving comets indicate plus-end-distal microtubules, whereas retrogradely-moving comets indicate minus-end-distal microtubules. Before the introduction of this method (Stepanova *et al.*, 2003), the polarity orientation of axonal microtubules was thought to be perfectly or almost perfectly uniform (Baas *et al.*, 1988; Heidemann, 1991). The EB3 method has revealed that developing axons in culture can sometimes display surprising numbers of minus-end-distal microtubules. The existence of some minus-end-distal of microtubules in shorter axons of cultured neurons probably reflects their immaturity, as longer more established axons in culture actually do display over 90% plus-end-distal microtubules (see Hasaka *et al.*, 2004; where 96.3% of axonal microtubules were plus-end-distal). Moreover, in studies in which the comets were observed in an intact animal, the microtubules in the axon were revealed to be completely plus-end-distal (Zheng *et al.*, 2008). In light of these observations, it is interesting that addition of bFGF to our cultures resulted in a notable uptick in the numbers of retrogradely-moving comets. This was particularly accentuated in the parent axon at sites giving rise to new branches, although no minus-end-distal microtubules were observed in the newly forming branches themselves. We suspect that the transient presence of higher numbers of minus-end-distal microtubules in axons represents moments of enhanced plasticity, when the axon is undergoing rapid morphological changes, such as branch formation.

We recognize that axonal branch formation involves critical changes in membrane trafficking and the actin cytoskeleton, not just microtubules. However, it has been reported that local reduction in microtubule mass results in the addition of new membrane to the axon (Zakharenko and Popov, 1998), and it is known that plus ends of microtubules interact with a wide variety of proteins that impact the cortical actin cytoskeleton (Kornack and Giger, 2005). Thus, we would contend that alterations in microtubule severing may be upstream to the various other cellular events important for interstitial branches to form. If this is correct, alterations in microtubule severing would be the seminal event in the formation of axonal branches.

ACKNOWLEDGMENTS

We thank Dr. Niels Galjart for the EB3 construct and Dr. Lester Binder for the tau antibodies. This work was supported by grants to P.W.B. from the National Institutes of Health, the National Science Foundation, the Spastic Paraplegia Foundation, the State of Pennsylvania Tobacco Settlement Funds, and the Craig H. Neilsen Foundation and also by a grant to W.Y. from the Craig H. Neilsen Foundation.

REFERENCES

Ahmad, F. J., He, Y., Myers, K. A., Hasaka, T. P., Francis, F., Black, M. M., and Baas, P. W. (2006). Effects of dynactin disruption and dynein depletion on axonal microtubules. Traffic *7*, 524–537.

Ahmad, F. J., Yu, W., McNally, F. J., and Baas, P. W. (1999). An essential role for katanin in severing microtubules in the neuron. J. Cell Biol. *145*, 305–315.

Aletsee, C., Brors, D., Mlynski, R., Ryan, A. F., and Dazert, S. (2003). Branching of spiral ganglion neurites is induced by focal application of fibroblast growth factor-1. Laryngoscope *113*, 791–796.

Baas, P. W., Deitch, J. S., Black, M. M., and Banker, G. A. (1988). Polarity orientation of microtubules in hippocampal neurons: uniformity in the axon and nonuniformity in the dendrite. Proc. Natl. Acad. Sci. USA *85*, 8335–8339.

Baas, P. W., Karabay, A., and Qiang, L. (2005). Microtubules cut and run. Trends Cell Biol. *15*, 518–524.

Baas, P. W., Vidya Nadar, C., and Myers, K. A. (2006). Axonal transport of microtubules: the long and short of it. Traffic *7*, 490–498.

Berry, R. W., *et al.* (2004). Tau epitope display in progressive supranuclear palsy and corticobasal degeneration. J. Neurocytol. *33*, 287–295.

Binder, L. I., Frankfurter, A., and Rebhun, L. I. (1985). The distribution of tau in the mammalian central nervous system. J. Cell Biol. *101*, 1371–1378.

Claudiani, P., Riano, E., Errico, A., Andolfi, G., and Rugarli, E. I. (2005). Spastin subcellular localization is regulated through usage of different translation start sites and active export from the nucleus. Exp. Cell Res. *309*, 358–369.

Connell, J. W., Lindon, C., Luzio, J. P., and Reid, E. (2008). Spastin couples microtubule severing to membrane traffic in completion of cytokinesis and secretion. Traffic *10*, 42–56.

Dawson, H. N., Ferreira, A., Eyster, M. V., Ghoshal, N., Binder, L. I., and Vitek, M. P. (2001). Inhibition of neuronal maturation in primary hippocampal neurons from tau deficient mice. J. Cell Sci. *114*, 1179–1187.

Dent, E. W., Barnes, A. M., Tang, F., and Kalil, K. (2004). Netrin-1 and semaphorin 3A promote or inhibit cortical axon branching, respectively, by reorganization of the cytoskeleton. J. Neurosci. *24*, 3002–3012.

Dent, E. W., Callaway, J. L., Szebenyi, G., Baas, P. W., and Kalil, K. (1999). Reorganization and movement of microtubules in axonal growth cones and developing interstitial branches. J. Neurosci. *19*, 8894–8908.

Dent, E. W., and Kalil, K. (2001). Axon branching requires interactions between dynamic microtubules and actin filaments. J. Neurosci. *21*, 9757–9769.

Falnikar, A., and Baas, P.W. (2009). Critical roles for microtubules in axonal development and disease. Results Probl. Cell Differ. *48*, 47–64.

Hartman, J. J., and Vale, R. D. (1999). Microtubule disassembly by ATP-dependent oligomerization of the AAA enzyme katanin. Science *286*, 782–785.

Hasaka, T. P., Myers, K. A., and Baas, P. W. (2004). Role of actin filaments in the axonal transport of microtubules. J. Neurosci. *24*, 11291–11301.

He, Y., Francis, F., Myers, K. A., Yu, W., Black, M. M., and Baas, P. W. (2005). Role of cytoplasmic dynein in the axonal transport of microtubules and neurofilaments. J. Cell Biol. *168*, 697–703.

Heidemann, S. R. (1991). Microtubule polarity determination based on formation of protofilament hooks. Methods Enzymol. *196*, 469–477.

Joshi, H. C., and Baas, P. W. (1993). A new perspective on microtubules and axon growth. J. Cell Biol. *121*, 1191–1196.

Karabay, A., Yu, W., Solowska, J. M., Baird, D. H., and Baas, P. W. (2004). Axonal growth is sensitive to the levels of katanin, a protein that severs microtubules. J. Neurosci. *24*, 5778–5788.

Klimaschewski, L., Nindl, W., Feurle, J., Kavakebi, P., and Kostron, H. (2004). Basic fibroblast growth factor isoforms promote axonal elongation and branching of adult sensory neurons in vitro. Neuroscience *126*, 347–353.

Kornack, D. R., and Giger, R. J. (2005). Probing microtubule +TIPs: regulation of axon branching. Curr. Opin. Neurobiol. *15*, 58–66.

Lee, H. H., Jan, L. Y., and Jan, Y. N. (2009). Drosophila IKK-related kinase Ik2 and Katanin p60-like 1 regulate dendrite pruning of sensory neuron during metamorphosis. Proc. Natl. Acad. Sci. USA *106*, 6363–6368.

Mancuso, G., and Rugarli, E. I. (2008). A cryptic promoter in the first exon of the SPG4 gene directs the synthesis of the 60-kDa spastin isoform. BMC Biol. *6*, 31.

Mandell, J. W., and Banker, G. A. (1996). A spatial gradient of tau protein phosphorylation in nascent axons. J. Neurosci. *16*, 5727–5740.

McNally, K.P., Bazirgan, O.A., and McNally, F.J. (2000). Two domains of p80 katanin regulate microtubule severing and spindle pole targeting by p60 katanin. J. Cell Sci. *113*(Pt 9), 1623–1633.

Myers, K. A., and Baas, P. W. (2007). Kinesin-5 regulates the growth of the axon by acting as a brake on its microtubule array. J. Cell Biol. *178*, 1081–1091.

Myers, K. A., Tint, I., Nadar, C. V., He, Y., Black, M. M., and Baas, P. W. (2006). Antagonistic forces generated by cytoplasmic dynein and myosin-II during growth cone turning and axonal retraction. Traffic *7*, 1333–1351.

Nadar, V. C., Ketschek, A., Myers, K. A., Gallo, G., and Baas, P. W. (2008). Kinesin-5 is essential for growth-cone turning. Curr. Biol. *18*, 1972–1977.

Papasozomenos, S. C., and Binder, L. I. (1987). Phosphorylation determines two distinct species of Tau in the central nervous system. Cell Motil. Cytoskelet. *8*, 210–226.

Pujol, F., Kitabgi, P., and Boudin, H. (2005). The chemokine SDF-1 differentially regulates axonal elongation and branching in hippocampal neurons. J. Cell Sci. *118*, 1071–1080.

Qiang, L., Yu, W., Andreadis, A., Luo, M., and Baas, P. W. (2006). Tau protects microtubules in the axon from severing by katanin. J. Neurosci. *26*, 3120–3129.

Riano, E., *et al.* (2009). Pleiotropic effects of spastin on neurite growth depending on expression levels. J. Neurochem. *108*, 1277–1288.

Solowska, J. M., Morfini, G., Falnikar, A., Himes, B. T., Brady, S. T., Huang, D., and Baas, P. W. (2008). Quantitative and functional analyses of spastin in the nervous system: implications for hereditary spastic paraplegia. J. Neurosci. *28*, 2147–2157.

Stepanova, T., Slemmer, J., Hoogenraad, C. C., Lansbergen, G., Dortland, B., De Zeeuw, C. I., Grosveld, F., van Cappellen, G., Akhmanova, A., and Galjart, N. (2003). Visualization of microtubule growth in cultured neurons via the use of EB3-GFP (end-binding protein 3-green fluorescent protein). J. Neurosci. *23*, 2655–2664.

Szebenyi, G., Dent, E. W., Callaway, J. L., Seys, C., Lueth, H., and Kalil, K. (2001). Fibroblast growth factor-2 promotes axon branching of cortical neurons by influencing morphology and behavior of the primary growth cone. J. Neurosci. *21*, 3932–3941.

Tarrade, A., *et al.* (2006). A mutation of spastin is responsible for swellings and impairment of transport in a region of axon characterized by changes in microtubule composition. Hum. Mol. Genet. *15*, 3544–3558.

Wang, K. H., Brose, K., Arnott, D., Kidd, T., Goodman, C. S., Henzel, W., and Tessier-Lavigne, M. (1999). Biochemical purification of a mammalian slit protein as a positive regulator of sensory axon elongation and branching. Cell *96*, 771–784.

Wang, L., and Brown, A. (2002). Rapid movement of microtubules in axons. Curr. Biol. *12*, 1496–1501.

Wu, X., Xiang, X., and Hammer, J. A., 3rd (2006). Motor proteins at the microtubule plus-end. Trends Cell Biol. *16*, 135–143.

Yu, W., Ahmad, F. J., and Baas, P. W. (1994). Microtubule fragmentation and partitioning in the axon during collateral branch formation. J. Neurosci. *14*, 5872–5884.

Yu, W., Qiang, L., and Baas, P. W. (2007). Microtubule-severing in the axon: implications for development, disease, and regeneration after injury. J. Environ. Biomed. *1*, 1–7.

Yu, W., Qiang, L., Solowska, J. M., Karabay, A., Korulu, S., and Baas, P. W. (2008). The microtubule-severing proteins spastin and katanin participate differently in the formation of axonal branches. Mol. Biol. Cell *19*, 1485–1498.

Yu, W., Solowska, J. M., Qiang, L., Karabay, A., Baird, D., and Baas, P. W. (2005). Regulation of microtubule severing by katanin subunits during neuronal development. J. Neurosci. *25*, 5573–5583.

Zakharenko, S., and Popov, S. (1998). Dynamics of axonal microtubules regulate the topology of new membrane insertion into the growing neurites. J. Cell Biol. *143*, 1077–1086.

Zhang, D., Rogers, G. C., Buster, D. W., and Sharp, D. J. (2007). Three microtubule severing enzymes contribute to the "Pacman-flux" machinery that moves chromosomes. J. Cell Biol. *177*, 231–242.

Zheng, Y., Wildonger, J., Ye, B., Zhang, Y., Kita, A., Younger, S. H., Zimmerman, S., Jan, L. Y., and Jan, Y. N. (2008). Dynein is required for polarized dendritic transport and uniform microtubule orientation in axons. Nat. Cell Biol. *10*, 1172–1180.